Research Article

Zeeshan Khan, Haroon Ur Rasheed, Murad Ullah, Ilyas Khan*, Tawfeeq Abdullah Alkanhal, and Iskander Tlili

Shooting method analysis in wire coating withdrawing from a bath of Oldroyd 8-constant fluid with temperature dependent viscosity

https://doi.org/10.1515/phys-2018-0117
Received Mar 16, 2018; accepted May 17, 2018

Abstract: The most important plastic resins used in wire coating are high/low density polyethylene (LDPE/HDPE), plasticized polyvinyl chloride (PVC), nylon and polysulfone. To provide insulation and mechanical strength, coating is necessary for wires. Simulation of polymer flow during wire coating dragged from a bath of Oldroyd 8-constant fluid incompresible and laminar fluid inside pressure type die is carried out numerically. In wire coating the flow depends on the velocity of the wire, geometry of the die and viscosity of the fluid.The non-dimensional resulting flow and heat transfer differential equations are solved numerically by Ruge-Kutta 4^{th}-order method with shooting technique. Reynolds model and Vogel's models are encountered for temperature dependent viscosity. The numerical solutions are obtained for velocity field and temperature distribution. The solutions are computed for different physical parameters.It is observed that the non-Newtonian propertis of fluid were favourable, enhancing the velocity in combination with temperature dependent variable. The Brinkman number contributes to increase the temperature for both Reynolds and Vogel'smodels. With the increasing of pressure gradient parameter of both Reynolds and Vogel's models, the velocity and temperature profile increases significantly in the presence of non-Newtonian parameter. Furthermore, the present result is also compared with published results as a particular case.

Keywords: Ruge-Kuta 4^{th}-order method, heat transfer, temperature dependent viscosity, wire coating, viscoelastic Oldroyd 8-constant fluid

PACS: 57.85.-g, 47.50.-d

1 Introduction

The understanding and analysis of non-Newtonian fluids is of great interest from fundamental as well as applied perspective [1, 2]. The knowledge of physics and material science associated with the flows of non-Newtonian fluids may have direct effects on numerous fields such as polymer preparation, covering and coating, ink-jet printing, smaller scale fluidics, homodynamics, the flow of turbulent shear, colloidal and additive suspensions, animal blood etc. For this reason, research has been concentrated on these flows and subsequently the literature presents extensive work on numerical, analytical, and asymptotic solutions on the subject [3, 4]. Furthermore, flow of these fluids presents great challenges equally to the experts from diverse research fields such as numerical simulations, engineering, mathematics, physics. Indeed, the equations proposed and created for non-Newtonian models are considerably more complicated, compared to those for Newtonian fluids. The modeled equations of non-Newtonian fluid are highly nonlinear and it is very difficult to obtain the exact solutions of such equations [5–8]. Due to the non-linear and inapplicable nature in terms of superposition principle, it is hard to obtain highly accurate solutions for viscous fluids [5–8]. For this purpose, many researchers developed analytical and numerical techniques to obtain the solutionstothese non-linear equations.

Wire-coating (an extrusion procedure) is generally utilized as a part of the polymer industry for insulation and it protects the wire from mechanical damage. In this pro-

***Corresponding Author: Ilyas Khan:** Faculty of Mathematics and Statistics, Ton Duc Thang University, Ho Chi Minh City, Vietnam; Email: ilyaskhan@tdt.edu.vn
Zeeshan Khan, Haroon Ur Rasheed: Sarhad University of Science and Information Technology, Peshawar, KP, 2500, Pakistan
Murad Ullah: Department of Mathematics, Islamia College University of Pesshawar, KP, 2500, Pakistan
Tawfeeq Abdullah Alkanhal: Department of Mechatronics and System Engineering, College of Engineering, Majmaah University, Majmaah 11952, Saudi Arabia
Iskander Tlili: Energy and Thermal Systems Laboratory, National Engineering School of Monastir, Street Ibn El Jazzar, 5019 Monastir, Tunisia

cedure an exposed preheated fiber or wire is dipped and dragged through the melted polymer. This procedure can also be accomplished by extruding the melted polymer over a moving wire. A typical wire coating equipment is composed of five distinct units: pay-off tool, wire preheating tool, an extruder, a cooling and a take-off tool. The most common dies used for coatings are tubing-type dies and pressure type dies. The latter is normally used for wire-coating and is shaped like an annulus. Flows through such die are therefore similar to the flows through an annular area formed by two coaxial cylinders. One of the two cylinders (inner cylinder) moves in the axial direction while the second (external cylinder) is fixed. Preliminary efforts by several researchers [9–14] used power-law and Newtonian models to reveal the rheology of the polymer melt flow. In references [15, 16], authors provide the wire coating analysis using pressure type die. Afterwards, more research regarding this matter was conveyed in references [17–20]. In addition, a very detailed survey regarding heat transfer and fluid flow in wire-coating is given in references [21–40]. Akter and Hashmi [42], analyzed the wire coating using pressurized die. Later on, Akter and Hashmi performed simulations on polymer flow during the wire-coating process by means of a conical unit as in references [43, 44].

Wire coating or covering is a modern industrial procedure to coat a wire for insulation and environmental safety. Wire coating can be classified in three types: dipping process, coaxial process, and electrostatic deposition process. The dipping process provides considerably stronger bond among the continuums however this process is relatively slow when compared to the other two processes. The problems related to the coating extrusion based on the pressure-die were reviewed by Han and Rao [45]. Generally, the extrusion process requires three components: the feeding unit, the barrel and a head with a die. Detailed discussions regarding these three distinct elements are reported by Kozan in reference [46]. In addition, Sajid *et al.* [47] addressed and solved the wire-coating process of Oldroyd (8-constant fluid) by utilizing HAM method. Similarly, Shah *et al.* [48] utilized the perturbation approach and analytically analyzed the wire-coating of a third-grade fluid.

At present, the Phan-Thien Tanner (PTT) model, a third-grade visco-elastic fluid model, is the most commonly used model for wire-coating. The high-speed wire-coating process for polymer melts in elastic constitutive model was analyzed by Binding in [49]. It also discussed the shortcomings of the realistic modeling approach. Multu *et al.* in [50] provided the wire-coating analysis based on the tube-tooling die. Kasajima and Ito in [51] analyzed the wire-coating process and examined the post treatment of polymer extruded. They also discussed the impacts of heat transfer on cooling coating. Afterward, Winter [52, 53] investigated the thermal effect on die both from Internal and external perspective. Recently, wire-coating in view of linear variations of temperature in the post-treatment analysis was investigated by Baag and Mishra [54].

Wet-on-dry (WOD) and wet-on-wet (WOW) are the most common coating process used for double-layer coating. In WOD processthe fiber is dragged into the primary layer and then curved by ultraviolet lamp. Then,primary coated layeris passed through the secondary coating-layer and again curved by ultraviolet lamp. But in the WOW process the fiber is passedfrom the primary and secondary-coating die and then curved by ultraviolet lamp. Recently WOW process gained significant importance production industry. Herein, WOW coating-process is applied for fiber optics. Kim *et al.* [55] used WOW process for the analysis of two-layers coating on optical fiber. Zeeshan *et al.* [56, 57] used pressure coating die for the two-layer coating in optical coating analysis using PTT fluid model. The same author discussed viscoelastic fluid for two-layer coating in fiber coating [58]. The Sisko fluid model was used for fiber coating by adopting WOW process by Zeeshan *et al.* [59] in the presence of pressure type coating die.

In the recent study MHD flow of viscoelastic Oldroyd 8-constant fluid is investigated for wireinside pressurized coating die. The modeled equations describing the polymer flow inside the die are solved numerically by Runge-Kutta Fehlberg algorithm with shooting technique [60–83]. The result is validated via a comparison with published results by Shah *et al.* [83].

2 Modeling of the problem

Thegeometry of the flow problem isshown in Figure 1 in which thewire of radius R_w is dragged with velocity V inside the coating die filled with viscoelastic fluid. The fluidis electrically conducted in the presence ofapplied magneticfield B_0 normal to the flow. Due to small magnetic Reynold number the inducedmagnetic field is negligible, which is also a valid assumption on a laboratory scale.

The velocity and temperature profiles for one-dimensional flow are

$$u = [0, 0, w(r)], \mathbf{S} = \mathbf{S}(r), \Theta = \Theta(r). \tag{1}$$

Here R_d is the radius of the die, θ_w temperature of the wire and θ_d is the temperature of the die.

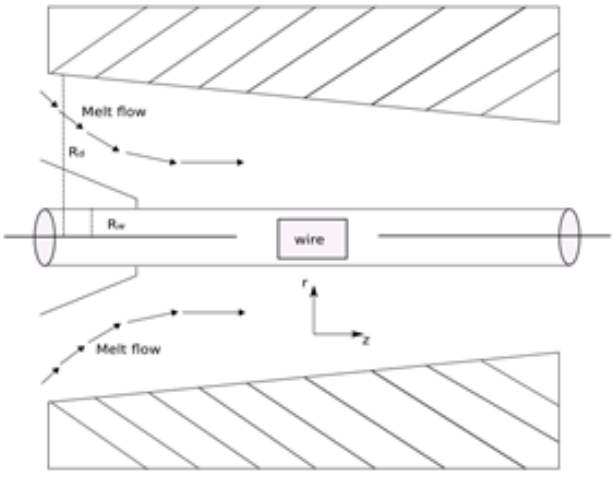

Figure 1: Geometry of wire coating process

For viscoelastic fluid, the stres tensor is:

$$\mathbf{S} + \gamma_1 \frac{D\mathbf{S}}{Dt} + \frac{\gamma_3}{2}(\mathbf{A}_1\mathbf{S} + \mathbf{S}\mathbf{A}_1) + \frac{\gamma_5}{2}(tr\mathbf{S})\mathbf{A}_1 + \frac{\gamma_6}{2}(tr\mathbf{S}\mathbf{A}_1)\mathbf{I} = \eta\left(\mathbf{A}_1 + \gamma_2\frac{D\mathbf{A}_1}{Dt} + \gamma_4\mathbf{A}_1^2 + \frac{\gamma_7}{2}\left(tr\mathbf{A}_1^2\right)\mathbf{I}\right), \tag{2}$$

In above equation $\mathbf{A}_1$ and $\gamma_i\,(i = 1-7)$ are the Rivlin-Ericksen tensor and material constants, respectively.

$$\mathrm{A}_1 = L^T + L, \tag{3}$$

$$\mathrm{A}_n = \mathrm{A}_{n-1}L^T + L\mathrm{A}_{n-1} + \frac{D\mathrm{A}_{n-1}}{Dt}, n = 2, 3, \ldots \tag{4}$$

The basic governing equations for incompressible flow are the continuity, momentum and energy equations, given by:

$$\nabla.u = 0, \tag{5}$$

$$\rho\frac{Du}{Dt} = \nabla.\mathrm{T} + \mathrm{J}\times\mathrm{B}, \tag{6}$$

$$\rho c_p\frac{D\theta}{Dt} = k\nabla^2\theta + \mathrm{T.L}, \tag{7}$$

In Eq. (6) the body force is defined as:

$$\mathrm{J}\times\mathrm{B} = (0, 0, -\sigma B_0^2 w). \tag{8}$$

In view of Eqs. (1)-(7), we have:

$$\frac{\partial p}{\partial r} = \frac{1}{r}\frac{d}{dr}(rS_{rz}), \tag{9}$$

$$\frac{\partial p}{\partial \theta} = 0, \tag{10}$$

$$\frac{\partial p}{\partial z} = \frac{1}{r}\frac{d}{dr}(rS_{rz}) - \sigma B_0^2 w - \frac{\nu}{k_p}w, \tag{11}$$

$$\frac{\partial p}{\partial z} = \frac{1}{r}\frac{d}{dr}\left[\frac{r\eta\left(1+\alpha\left(\frac{dw}{dr}\right)^2\right)}{\left(1+\beta\left(\frac{dw}{dr}\right)^2\right)}\right], \tag{12}$$

$$k\left(\frac{d^2\theta}{dr^2} + \frac{1}{r}\frac{d\theta}{dr}\right)\left[\frac{r\eta\left(1+\alpha\left(\frac{dw}{dr}\right)^2\right)}{\left(1+\beta\left(\frac{dw}{dr}\right)^2\right)}\right] = 0, \tag{13}$$

where

$$\alpha = \gamma_1(\gamma_4+\gamma_7) - (\gamma_3+\gamma_5)(\gamma_4+\gamma_7-\gamma_2) - \frac{\gamma_5\gamma_7}{2},$$
$$\beta = \gamma_1(\gamma_3+\gamma_6) - (\gamma_3+\gamma_5)\gamma_1(\gamma_3+\gamma_6-\gamma_1) - \frac{\gamma_5\gamma_6}{2}.$$

2.1 Constant viscosity

Introducing the dimensionless parameters:

$$r^* = \frac{r}{R_w}, w^* = \frac{w}{V}, \alpha^* = \frac{\alpha V^2}{R_w^2}, \beta^* = \frac{\beta V^2}{R_w^2}, \tag{14}$$
$$M = \frac{\sigma B_0^2}{(\eta/R_w^2)}, p^* = \frac{p}{(\eta V/R_w^2)}, k_p^* = \frac{R_w^2}{Vk_p},$$
$$\theta^* = \frac{\theta-\theta_w}{\theta_d-\theta_w}, Br = \frac{\eta V^2}{k(\theta_d-\theta_w)}, \frac{\partial p}{\partial r} = \Omega$$

In view of Eq. (14), the system of Eqs. (12) and (13) becomes:

$$r\Omega = \frac{\left[\frac{dw}{dr} + (\alpha+\beta)\left(\frac{dw}{dr}\right)^3 + \alpha\beta\left(\frac{dw}{dr}\right)^5\right]}{\left[1+\beta\left(\frac{dw}{dr}\right)^2\right]^3} + \frac{r\left[\frac{d^2w}{dr^2} + (3\alpha-\beta)\left(\frac{dw}{dr}\right)^2\left(\frac{d^2w}{dr^2}\right) + \alpha\beta\left(\frac{dw}{dr}\right)^4\frac{d^2w}{dr^2}\right]}{\left[1+\beta\left(\frac{dw}{dr}\right)^2\right]^3} + \frac{1}{\eta}\frac{d\eta}{dr}r\left[\frac{\frac{dw}{dr}+\alpha\left(\frac{dw}{dr}\right)^3}{1+\beta\left(\frac{dw}{dr}\right)^2}\right] - \frac{1}{\eta}\left[Mwr + \frac{1}{Kp}wr\right], \tag{15}$$

$$\left[\frac{d^2\theta}{dr^2} + \frac{1}{r}\frac{d\theta}{dr}\right] + \frac{\eta\beta_r\left(\frac{dw}{dr}\right)^2\left[\left[1+\beta\left(\frac{dw}{dr}\right)^2\right]\right]}{\left[1+\beta\left(\frac{dw}{dr}\right)^2\right]} = 0 \tag{16}$$

Corresponding to the boundary-conditions

$$w(1) = 1 \tag{17}$$

$$\theta(1) = 0, \theta(\delta) = 1. \tag{18}$$

The constant viscosity case is discussed by Shah *et al.* [46] in detail. Here we discuss the variable viscosity case.

2.2 Reynolds model

In this case η is a function of temperature. Introducing the dimensionless parameters:

$$r^{\star}=\frac{r}{R_w}, w^{\star}=\frac{w}{V}, \alpha^{\star}=\frac{\alpha V^2}{R_w^2}, \frac{R_d}{R_w}=\delta>1, \quad (19)$$
$$\beta^{\star}=\frac{\beta V^2}{R_w^2}, M=\frac{\sigma B_0^2}{(\eta/R_w^2)}, p^{\star}=\frac{pR_w}{(\eta V)}, k_p^{\star}=\frac{R_w^2}{Vk_p},$$
$$\theta^{\star}=\frac{\theta-\theta_w}{\theta_d-\theta_w}, Br=\frac{\eta V^2}{k(\theta_d-\theta_w)}, \frac{\partial p}{\partial r}=\Omega.$$

In Reynolds model, the dimensionless temperature dependent viscosity can be expressed as $\eta=e^{(-\beta_0 m\theta)}\approx 1-\beta_0 m\theta$. Therefore, Eqs. (15)-(18) in view of Eq. (19) become:

$$\frac{d^2w}{dr^2}=\frac{r\left(1+\beta\left(\frac{dw}{dr}\right)^2\right)\cdot A}{r\left[1+(3\alpha-\beta)\left(\frac{dw}{dr}\right)^2+\alpha\beta\left(\frac{dw}{dr}\right)^4\right]} - \frac{\left[\frac{dw}{dr}+(\alpha+\beta)\left(\frac{dw}{dr}\right)^3+\alpha\beta\left(\frac{dw}{dr}\right)^5\right]}{r\left[1+(3\alpha-\beta)\left(\frac{dw}{dr}\right)^2+\alpha\beta\left(\frac{dw}{dr}\right)^4\right]}, \quad (20)$$

where

$$A=\left[\Omega+\frac{1}{(1-\beta_0 m\theta)}\left(M+\frac{1}{Kp}\right)w + \frac{1}{(1-\beta_0 m\theta)}\beta_0 m\left(\frac{d\theta}{dr}\right)\left(\frac{\frac{dw}{dr}+\alpha\left(\frac{dw}{dr}\right)^3}{\left(1+\beta\left(\frac{dw}{dr}\right)^2\right)}\right)\right]$$

$$\frac{d^2\theta}{dr^2}=-\frac{1}{r}\frac{d\theta}{dr} - (1-B_0 m\theta)\frac{B_r\left(\left(\frac{dw}{dr}\right)^2+\alpha\left(\frac{dw}{dr}\right)^4\right)}{\left(1+\beta\left(\frac{dw}{dr}\right)^2\right)}, \quad (21)$$

$$w(1)=1, w(\delta)=0, \quad (22)$$
$$\theta(0)=0, \theta(\delta)=1.$$

2.3 Vogel's model

Temperature dependent viscosity can be expressed as $\eta=\eta_0\exp\left(\frac{D}{B'+\theta}-\theta_w\right)$, by expanding

$$\eta=\Omega_1\left(1-\frac{D}{B'^2}\theta\right), \quad (23)$$

where $\Omega_1=\eta_0\exp\left(\frac{D}{B'}-\theta_w\right)$ and D, B' denotes the temperature dependent viscosity parameters of the Vogel's model. Therefore, Eqs. (15)-(18) in view of Eqs. (19) and (23) become:

$$\frac{d^2w}{dr^2}=\frac{r\left(1+\beta\left(\frac{dw}{dr}\right)^2\right)\cdot B}{r\left[1+(3\alpha-\beta)\left(\frac{dw}{dr}\right)^2+\alpha\beta\left(\frac{dw}{dr}\right)^4\right]} - \frac{\left[\frac{dw}{dr}+(\alpha+\beta)\left(\frac{dw}{dr}\right)^3+\alpha\beta\left(\frac{dw}{dr}\right)^3\right]}{r\left[1+(3\alpha-\beta)\left(\frac{dw}{dr}\right)^2+\alpha\beta\left(\frac{dw}{dr}\right)^4\right]}, \quad (24)$$

where

$$B=\left[\Omega+\frac{1}{\Omega_1\left(1-\frac{D}{B'^2}\theta\right)}\left(M+\frac{1}{Kp}\right)w + \frac{D}{B'^2}\left(\frac{d\theta}{dr}\right)\left(\frac{\frac{dw}{dr}+\alpha\left(\frac{dw}{dr}\right)^3}{\left(1+\beta\left(\frac{dw}{dr}\right)^2\right)}\right)\right]$$

$$\frac{d^2\theta}{dr^2}=-\frac{1}{r}\frac{d\theta}{dr} - \Omega_1\left(1-\frac{D}{B_1^2}\theta\right)\frac{B_r\left(\left(\frac{dw}{dr}\right)^2+\alpha\left(\frac{dw}{dr}\right)^4\right)}{\left(1+\beta\left(\frac{dw}{dr}\right)^2\right)}, \quad (25)$$

$$w(1)=1, w(\delta)=0, \quad (26)$$
$$\theta(0)=0, \theta(\delta)=1.$$

3 Numerical solution

The above system of equations is solved numerically by using fourth order Runge-Kutta method along with shooting technique. For this purpose the Eqs. (20-22) and (24-26) are transformed in to first order due to the higher order equation at $r=\delta$ (boundary-layer thickness) being unavailable. Then, the boundary value problem is solved by shooting method.

3.1 Numerical solution of Reynolds model

Eqs. (20) and (21) are solved numerically by Ruge-Kutta method corresponding to the boundary conditions (22) by considering:

$$z_1=w, z_2=\frac{dw}{dr}\text{and}z_3=\theta, z_4=\frac{d\theta}{dr}. \quad (27)$$

In view of Eq. (27), Eqs. (20) and (21) become:

$$z_2' = \frac{C \cdot \left(1+\beta z_2^2\right)^2 - \left[z_2 + (\alpha+\beta) z_2^3 + \alpha\beta z_2^5\right]}{r\left[1 + (3\alpha - \beta) z_2^2 + \alpha\beta z_2^4\right]}, \tag{28}$$

$$z_4' = -\frac{1}{r} z_4 - (1 - B_0 m\theta) \frac{B_r \left(z_2^2 + \alpha z_2^4\right)}{\left(1+\beta z_2^2\right)},$$

where

$$C = \left[r\left(\Omega + \frac{1}{(1-\beta_0 m\theta)}\left(M + \frac{1}{Kp}\right)\right) z_1 + \frac{1}{(1-\beta_0 m\theta)} \beta_0 m z_4 \left(\frac{z_2 + \alpha z_2^3}{\left(1+\beta z_2^2\right)}\right)\right]$$

with boundary conditions:

$$z_a(1) = 1, z_b(1) = 0, \quad z_a(2) = 0, z_b(2) = 1. \tag{29}$$

3.2 Numerical solution of Vogel's model

The numerical solution of Eqs. (24) and (25) with boundary conditions given in Eq. (26) can be obtained by considering $D = \beta_0 b$. The expression for the velocity and temperature profiles are:

$$z_2' = \frac{D \cdot \left(1+\beta z_2^2\right)^2 - \left[z_2 + (\alpha+\beta) z_2^3 + \alpha\beta z_2^5\right]}{r\left[1 + (3\alpha - \beta) z_2^2 + \alpha\beta z_2^4\right]}, \tag{30}$$

where

$$D = \left[r\left(\Omega + \frac{1}{\Omega_1\left(1 - \frac{D}{B_1^2}\theta\right)}\left(M + \frac{1}{Kp}\right)\right) z_1 + \frac{\frac{D}{B_1^2} z_4}{\Omega_1\left(1 - \frac{D}{B_1^2}\theta\right)} \left(\frac{z_2 + \alpha z_2^3}{\left(1+\beta z_2^2\right)}\right)\right]$$

$$z_4' = -\frac{1}{r} z_4 - \Omega_1 \left(1 - \frac{D}{B_1^2}\theta\right) \frac{B_r \left(z_2^2 + \alpha z_2^4\right)}{\left(1+\beta z_2^2\right)}, \tag{31}$$

with the specific boundary conditions

$$z_a(1) = 1, z_b(1) = 0, \quad z_a(2) = 0, z_b(2) = 1. \tag{32}$$

4 Analysis of the results

In this section the results are discussed derived on the theoretical basis. In the following subsection the figures illustrate how the fluid velocity and the temperature distribution vary in the pressure unit of the conical geometry for different physical parameter values such as dilatant constant (α), pseudoplastic constant (β), viscosity parameter of Reynolds model (m), Vogel's parameter (Ω_1), Brinkman number (Br), magnetic parameter (M) and porosity parameter (k_p). The numerical solutions have been calcultaed by fourth order Ruge-Kutta method along with shooting technique.

(a) Reynolds model

Figure 2 displays the velocity profile in the presence of porous matrix (k_p) by variation of magnetic parameter (M) and dilatant constant (α). The effect of dilatant constant on the velocity profile is significant. It is noticed that the velocity profile retards with the increasing values of dilatant constant but reverse effect is observed in the presence of k_p and $M = 0$. For $M = 2$, the situation becomes adverse. It is interesting to note that for $\alpha = 0.4$ the present result made significant agreement with the reported results [45] when $M = 0, \mathrm{k}_p = 0.2$. The impact of β on velocity varaition is depicted in Figure 3 in the absence of $M$and for fixed val-

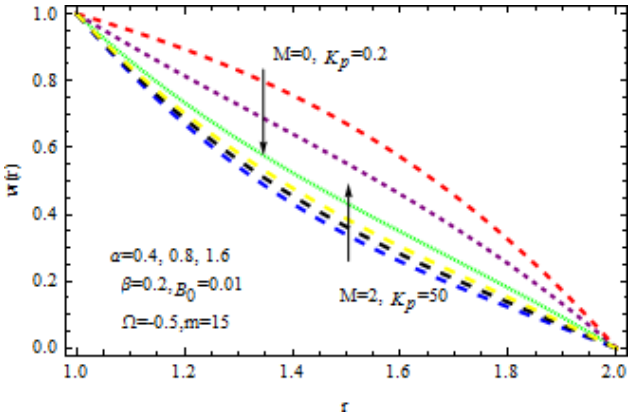

Figure 2: Impact of α on velocity (Reynolds model)

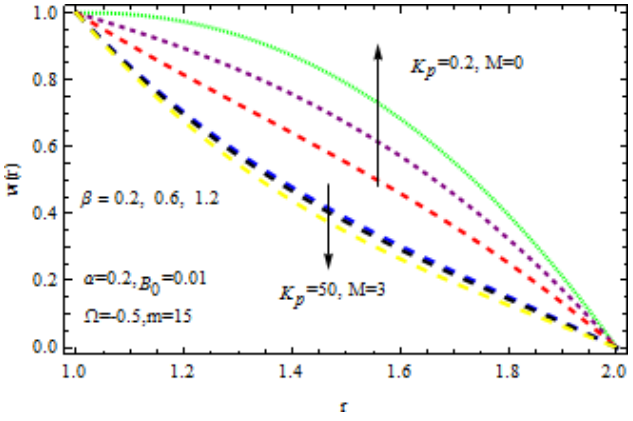

Figure 3: Impact of β on velocity (Reynolds model)

ues of k_p. It is observed that the pseudoplastic constant (β), accelerates the velocity of the coating polymer by taking $M = 0$. But converse effect is detected in the presence of k_p. It is also evident that for $M = 3$, the velocity profile retards as increases in the presence/absence of k_p.

Figure 4 displays the influence of viscosity parameter (Reynolds model parameter) m on the velocity profile. It is observed that for both presence of k_p and M the velocity profile increases all points. Due to high magnetic field, the electromagnetic force may add to nonlinearity of velocity distribution. It is also found that for high values of viscosity and magnetic parameter *i.e.*, $k_p = 50$ and $M = 2$, accelerates/decelerates the velocity profile. Figure 5 delineates the impact of M on velocity profile for two different values of k_p. It is perceived that the velocity profile decreases with magnetic parameter. This deceleration in velocity field is due to the Lorenz forces. In the presence and absence of M, Figure 6 depicts the velocity profile for various values of porous matrix. This shows that the porous matrix has accelerating effect of velocity profile both in the presence and absence of M. The impact of Br and M in the temperature profile is revealed in Figure 7. It follows that the Br *i.e.*, the relation between viscous heating andthe heat conductor, enhances the temperature distribution. It is also remarkable to note that two-layer variation is noted with the increasing values of magnetic parameter. Temperature distribution increases sharply within the region $r \leq 1.4$, and retards significantly. For $k_p = 0.2$ and 50, the impact of M and β on the temperature distribution is displayed in Figure 8. The Reynolds model viscosity parameter is taken to be fixed at $m = 15$. It is seen that the temperature decreases with increasing β in the presence/absence of M. Figure 9 shows the effect of porous matrix on temperature distribution. It is noticed that the temperature profile gets a higher gradient as $k_p$increase in both ceases. Also is remarkable to note that for large values of magnetic parameter and Brinkman number *i.e.*, $M = 3$ and $Br = 15$, the temperature is maximum at the middle of the annular die.

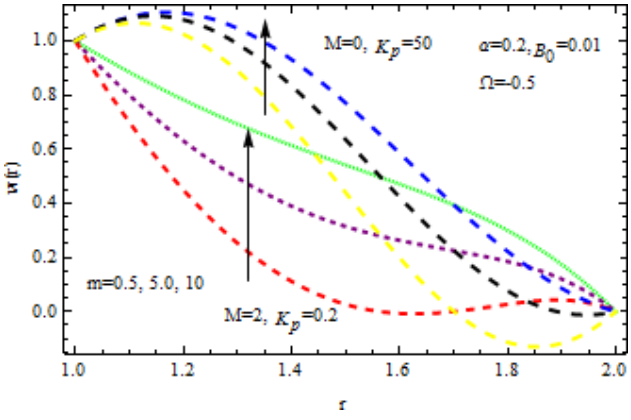

Figure 4: Impact of m on velocity (Reynolds model)

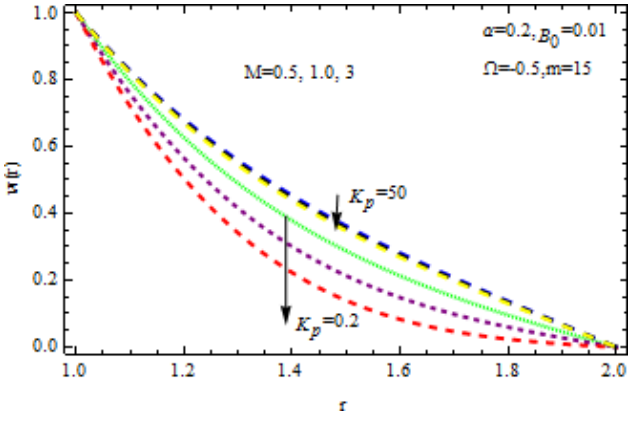

Figure 5: Impact of on velocity (Reynolds model)

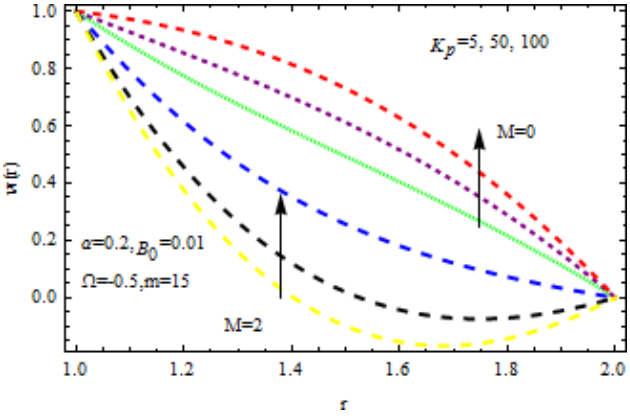

Figure 6: Impact of k_p on velocity (Reynolds model)

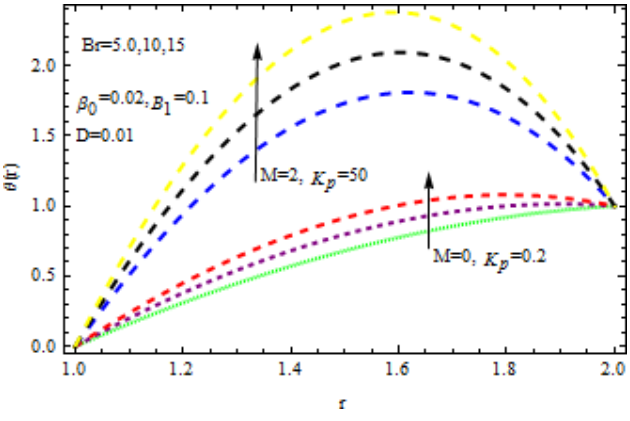

Figure 7: Impact of Br on temperature (Reynolds model)

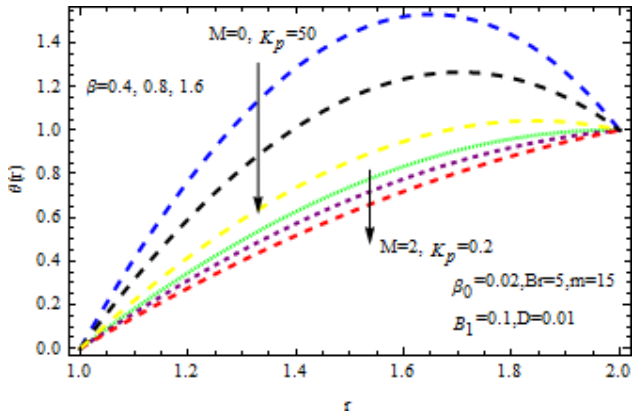

Figure 8: Impact of β on temperature (Reynolds model)

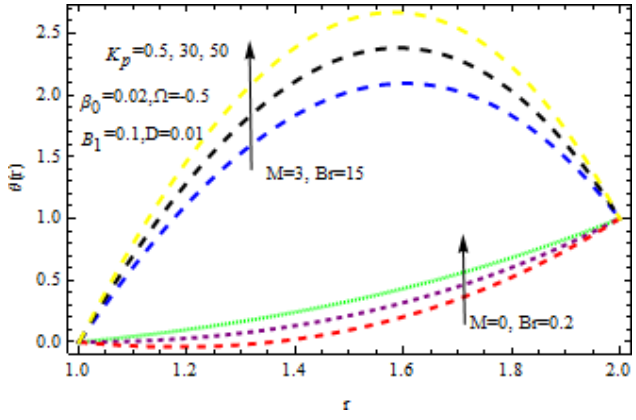

Figure 9: Impact of k_p on temperature (Reynolds model)

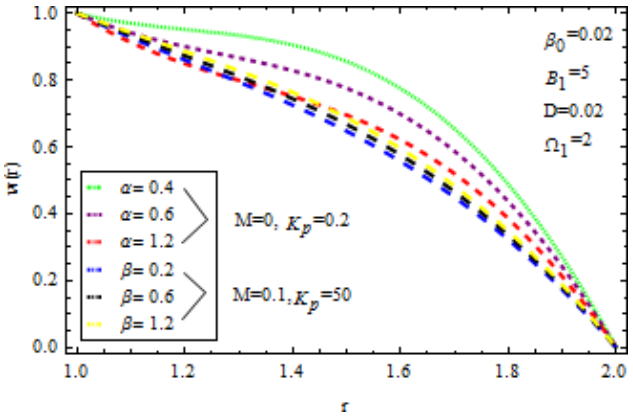

Figure 10: Impact of α and β on velocity (Vogel's model)

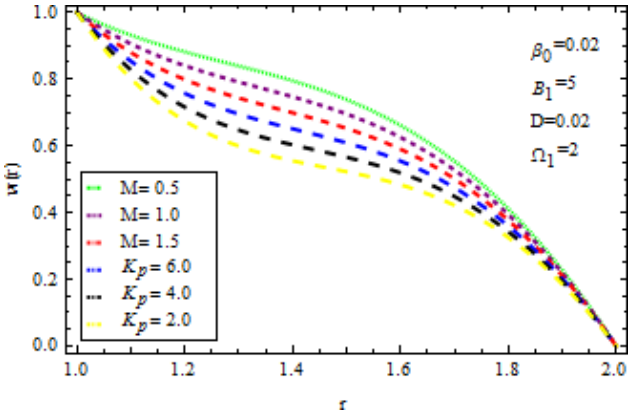

Figure 11: Impact of M and k_p on velocity (Vogel's model)

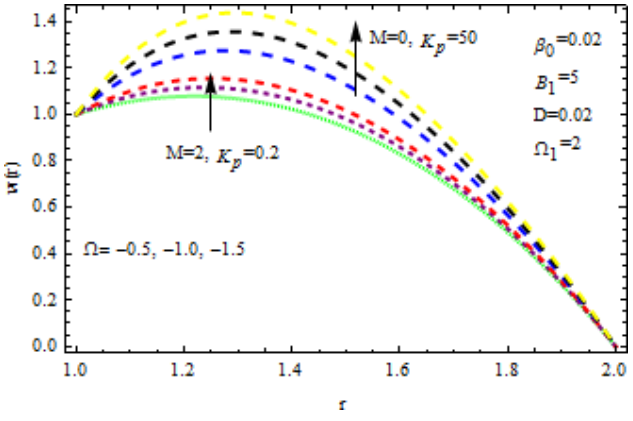

Figure 12: Impact of Ω on velocity profile (Vogel's model)

(b) Vogel's model

The effect of physical parameter involves in the Vogel's model on the solutions are revealed in Figures 10-16. Figure 10 shows the effect of the dilatant constant α as well as the pseudoplastic constant β in the presence/absence of M for fixed values of k_p = 0.2 and 50, on the velocity. From this simulation it is pointed out that the velocity decreases as the dilatant constant increases while the effect of β is opposite to that of α. Also the results of Shah *et al.* [45] can be easily recovered by taking $M = 0, k_p = 0, \alpha = 0.4$.

The variation of the velocity of the coating liquid is displayed in Figure 11. It is seen that the velocity decreases with increasing M. This due the Lorenz forces, which act as a resistive force and resist the motion of the fluid. The variation of the velocity is significant for porous matrix. Figure 12 depicts the effect of M and Ω_1 (pressure gradient parameter of Vegel's model) on the velocity profile. Due the existence of non-Newtonian characteristics the pressure gradient parameter accelerates the velocity profile significantly in the domain $r \leq 1.3$ and then decreases sharply. In the presence/absence of magnetic parameter M, the effect of pseudoplastic constanton temperature is displayed in Figure 13. With increasing β, the temperature distribution within the die increases. It is interesting to note that for $M = 3$ and $k_p = 0.2$, the temperature profile increases significantly inthe region $r \leq 1.5$ and afterwards, it decreases. Figure 14 reveals the effect of pressure gradient parameter of Vogel's model on the temperature profile with the contri-

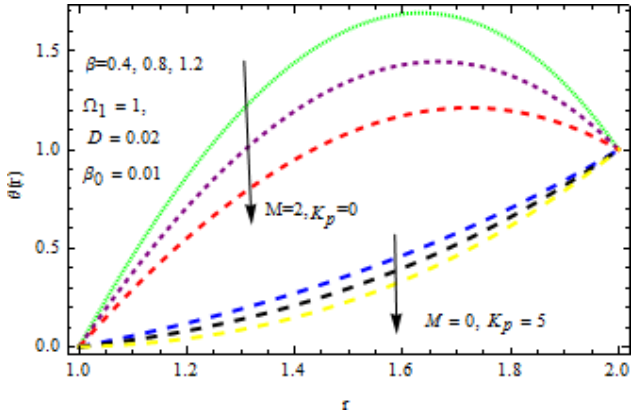

Figure 13: Impact of β on temperature (Vogel's model)

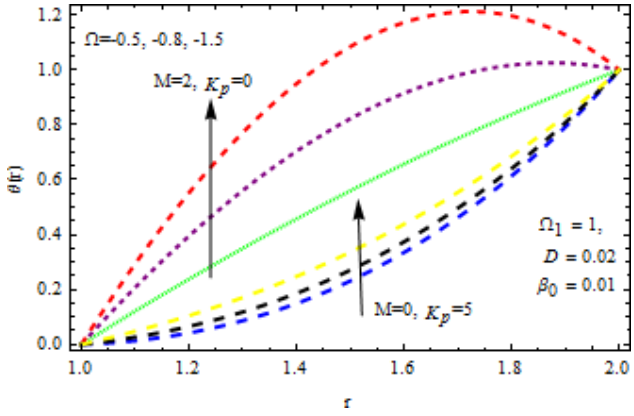

Figure 14: Impact of Ω on temperature (Vogel's model)

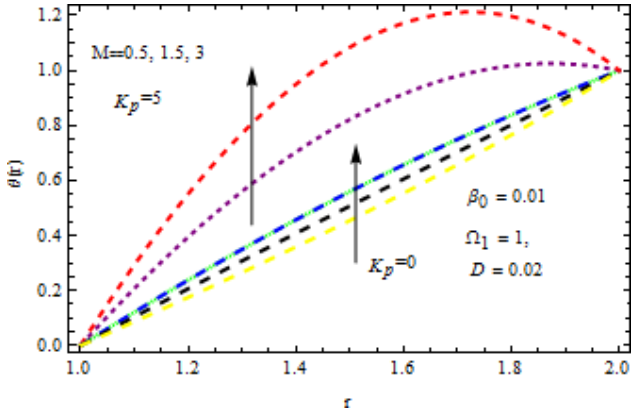

Figure 15: Impact of M on temperature (Vogel's model)

bution of constant porous matrix in the presence/absence of M. From this simulation it is observed that for$M = 0$ and $k_p = 0.2$, the temperature profile increases as Ω increases. A retarding effect was observed after the region $r \geq 1.5$ and in the presence of and k_p the reverse effect was encountered near the plate. An interesting observation is given in Figure 15. It is significant that the temperature distribution gets accelerated due to the increase of M in the presence. The impact of on the temperature is depicted in Figure 16. It is observed that for large value of Brinkman number *i.e.*, $Br = 20$, the peak in temperature distribution is encountered within the layer $1 \leq r \leq 1.7$ and afterwards, it decreased sharply in the presence of k_p. Finally, the present result is also validated by comparing with reported results [45] and good agreement is found as presented in Table 1.

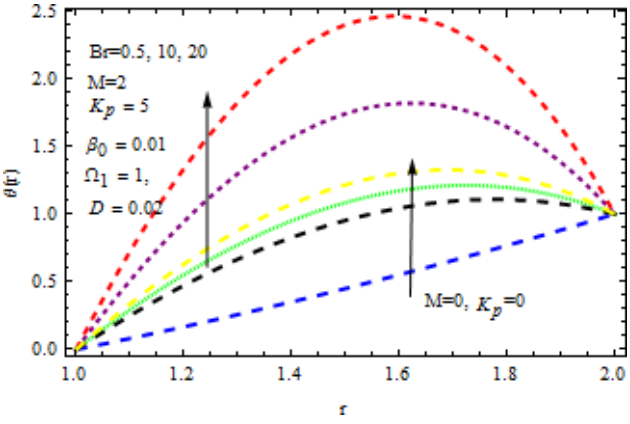

Figure 16: Impact of Br on temperature (Vogel's model)

Table 1: Comparison of present work with Rehan *et al.* [45]

r	Present work	Rehan *et al.* [45]
1	1	1
1.2	0.734425	0.73451
1.4	0.525222	0.525203
1.6	0.348501	0.348552
1.8	0.180476	0.180466
2	0	1

5 Conclusion

The magnetic field and heat transfer effect on wire coating analysis is investigated numerically while with drawing the wire from the center of he die filled with viscoelastic Oldroyd 8-constant fluid. The velocity and temperature profiles have been obtained numerically by applying Runge-Kutta 4^{th}-order method along with shooting technique. The effect of variable viscosity is also investigated. Reynolds and Vogel's models are used for the variable

viscosity. The effect of physical parameters such as values such as dilatant constant pseudoplastic constant (β), viscosity parameter of Reynolds model (m), and viscosity parameter of Vogel's model (Ω_1), Brinkman number magneticpparameter (M) and porosity parameter (k_p). It is seen that the non-Newtonian parameter of viscoelastic Oldroyd 8-constant fluid accelerates the velcity profile in the presence of porous matrix and $M = 0$. For large value of magnetic parameter the reverse effect is observed. It is observed that the temperature profiles decreases with increasing psedoplastic parameter in the presence and absence of magnetic parameter. The Brinkman number contributes to increase the temperature for both Reynolds and Vogel'smmodels. With increasing pressure gradient parameter with both Reynolds and Vogel's models, the velocity and temperature profile increases significantly in the presence of non-Newtonian parameter.

References

[1] Rajagopal., K.R. On the boundary conditions for fluids of the differential type, in: A. Sequira (Ed.), Navier-Stokes Equation and Related Non-Linear Problems, Plenum press, New York, 1995, 273-278.

[2] Rajagopal K.R., Kaloni. P.N., Some remarks on the boundary conditions for fluids of the differential type, in: G.A. Gram, S.K. Malik (Eds.), Continuum Mechanics and its Applications, Hemisphere, Washington DC, 1980, 935-941.

[3] Szeri A.Z., Rajagopal. K.R, Flow of a non-Newtonian fluid between heated parallel plates, Int. J. Non-Lin. Mech., 1985, 20, 91-101.

[4] Makinde O.D., Irreversibility analysis for gravitry driven non-Newtonian liquid film along an inclined isothermal plate, Phys. Scripta, 2006, 74, 642-645..

[5] Makinde O.D, Thermal criticality for a reactive gravity driven thin film flow of a third-grade fluid with adiabatic free surface down an inclined plane, Appl. Math. Mech. Ed., 2009, 30, 373-380.

[6] Massoudi M., Christie I., Effects of variable viscosity and viscous dissipation on the flow of a third-grade fluid in a pipe, Int. J. Non-Lin. Mech., 1995, 30, 687-699.

[7] Damirel Y., Kahraman R., Thermodynamics Analysis of Convective Heat Transfer in an Annular Packed Bed, Int. J. Heat Fluid Flow, 2000, 21, 442-448.

[8] Postelnicu A., Grosan T., Pop I., Free convection boundary-layer over a vertical permeable flat plate in a porous medium with internal heat generation, Int. Comm. Heat and Mass Trans., 2000, 27, 729-738.

[9] Bernhardt E.C., Processing of Thermoplastic Materials, Reinhold Publishing, New York, 1962, 263-269.

[10] McKelvey J.M., Polymer Processing, 1962, John Wiley and Sons, New York.

[11] Bagley E.B., Storey S.H., Processing of thermoplastic materials, WireWire Prod., 1963, 38, 1104-1122.

[12] Han C.D., Rao D., The rheology of wire coating extrusion, Polym. Eng. Sci.,1978, 18, 1019-1029.

[13] Carley J.F., Endo T., Krantz W., Realistic analysis of flow in wire coating dies,Polym. Eng. Sci.,1979, 19, 1178-1187.

[14] Han C.D., Rheology and Processing of Polymeric Materials Volume 2 Polymer Processing, Oxford University Press, 2007, 2, 235-256.

[15] Middleman S., Fundamentals of Polymer Processing, McGraw-Hill, New York,1977.

[16] Tadmor Z., Gogos C.G., Principle of Polymer Processing, 1978, John Wiley and Sons, New York.

[17] Kasajima M., Ito K., Post-treatment of polymer extrudate in wire coating, Appl.Polym. Symp., 1973, 221, 221-235.

[18] Tadmor Z., Bird R.B., Rheological analysis of stabilizing forces in wire-coating dies, Polym. Eng. Sci., 1974, 14,124-136.

[19] Caswell B., Tanner R.J., Wire coating die using finite element methods, Polym.Eng. Sci., 1985, 18, 417-421.

[20] Wagner R., Mitsoulis E., Effect of die design on the analysis of wire coating,Adv.Polym. Technol., 1985, 5, 305-325.

[21] Tlili I., Timoumi Y., Ben Nasrallah S., Numerical simulation and losses analysis in a Stirling engine, Int. J. Heat & Techn., 2006, 24, 1.

[22] Tlili I., Timoumi Y., Ben Nasrallah S., Thermodynamic analysis of Stirling heat engine with regenerative losses and internal irreversibilities, Int. J. Engine Res., 2007, 9, 45-56.

[23] Tlili I., Timoumi Y., Ben Nasrallah S., Performance optimization of Stirling engines', Renew. Ener., 2008, 33, 2134-2144.

[24] Ahmadi M.H., Ahmadi M.A., Pourfayaz F., Hosseinzade H., Acıkkalp E., Tlili I., Feidt M., Designing a powered combined Otto and Stirling cycle power plant through multi-objective optimization approach, Renew. Sust. Ener. Rev, May 2016.

[25] Tlili I., Renewable energy in Saudi Arabia: current status and future potentials, Environment, development and sustainability, 2015, 17, 4, 859-886.

[26] Sa'ed A., Tlili I., Numerical Investigation of Working Fluid Effect on Stirling Engine Performance, Int. J. Therm. Envir. Eng., 2015, 10, 1, 31-36.

[27] Tlili I., Finite time thermodynamic evaluation of endoreversible Stirling heat engine at maximum power conditions, Renew. Sust. Ener. Rev., May 2012.

[28] Tlili I., Thermodynamic Study On Optimal Solar Stirling Engine Cycle Taking Into Account The Irreversibilities Effects, Ener. Procedia, March 2012.

[29] Tlili I., A numerical investigation of an alpha Stirling engine, Int. J. Heat & Techn., July 2012.

[30] Tlili I., Musmar S.A., Thermodynamic evaluation of a second order simulation for Yoke Ross Stirling engine, Ener. Conv. Manag., April 2013.

[31] Tlili I., Timoumi Y., Nasrallah S.B., Analysis and design consideration of mean temperature differential Stirling engine for solar application, Renew. Ener., 2008, 33, 1911-1921.

[32] Timoumi Y., Tlili I., Nasrallah S.B., Design and performance optimization of GPU-3 Stirling engines, Energy, 2008, 33, 1100-1114.

[33] Timoumi Y., Tlili I., Nasrallah S.B., Reduction of energy losses in a Stirling engine" Heat Techn. 2007, 25(1), 84-93.

[34] Al-Qawasmi A.-R., Tlili I., Energy Efficiency Audit Based on Wireless Sensor and Actor Networks: Air-Conditioning Investigation, J. Eng., 2018, 3640821.

[35] Al-Qawasmi A.-R., Tlili I., Energy efficiency and economic impact investigations for air-conditioners using wireless sensing and

actuator networks, Ener. Rep., 2018, 4, 478-485.
[36] MN Khan, WA Khan, Tlili I., Forced Convection of Nanofluid Flow Across Horizontal Elliptical Cylinder with Constant Heat Flux Boundary Condition, J. Nanofluids, 2019, 8(2), 386-393.
[37] Tlili I., Khan W.A., Ramadan K., MHD Flow of Nanofluid Flow Across Horizontal Circular Cylinder: Steady Forced Convection, J. Nanofluids, 2019, 8(1), 179-186.
[38] Afridi M.I., Tlili I., Qasim M., Khan I., Nonlinear Rosseland thermal radiation and energy dissipation effects on entropy generation in CNTs suspended nanofluids flow over a thin needle, Bound. Value Probl., 2018, 148.
[39] Almutairi M.M., Osman M., Tlili I., Thermal Behavior of Auxetic Honeycomb Structure: An Experimental and Modeling Investigation, ASME. J. Ener. Res. Technol., 2018, 140(12), 122904-122904.
[40] Li Z., Khan I., Shafee A., Tlili I., Asifa T., Energy transfer of Jeffery-Hamel nanofluid flow between non-parallel walls using Maxwell-Garnetts (MG) and Brinkman models, Ener. Rep., 2018, 4, 393-399.
[41] Khan M.N., Tlili I., Innovative thermodynamic parametric investigation of gas and steam bottoming cycles with heat exchanger and heat recovery steam generator: Energy and exergy analysis, Ener. Rep., 2018, 4, 497-506.
[42] Akter S., Hashmi M.S.J., Modelling of the pressure distribution within ahydrodynamic pressure unit: effect of the change in viscosity during drawingof wire coating, J. Mater. Process. Technol.,1998, 77, 32-36.
[43] Akter S., Hashmi M.S.J., Analysis of polymer flow in a conical coating unit: apower law approach, Prog. Org. Coat., 1999, 37, 15-22.
[44] Akter S., Hashmi M.S.J., Wire drawing and coating using a combined geometryhydrodynamic unit, J. Mater. Process. Technol. 178 (2006) 98-110.
[45] Han C.D., Rao D., The rheology of wire coating extrusion, Polym. Eng. Sci., 1978, 18, 1019-1029.
[46] Kozan R., Prediction of the coating thickness of wire coating extrusionprocesses using artificialneural network (ANN), Mod. Appl. Sci., 2009, 3,52.
[47] Sajid M., Siddiqui A.M., Hayat T., Wire coating analysis using MHD oldroyd8-constant fluid, Int. J. Eng. Sci., 2007, 45, 381-392.
[48] Shah R.A., Islam S., Ellahi M., Siddhiqui A.M., Harron T., Analytical solutions forheat transfer flows of a third grade fluid in post treatment of wire coating, Int. J. Phys. Sci., 2011, 6, 4213-4223.
[49] Binding D.M., Blythe A.R., Guster S., Mosquera A.A., Townsend P., Wester M.P., Modelling polymer melt flows in wire coating process, J. Non-Newton. Fluid Mech., 1996, 64, 191-206.
[50] Multu I., Twnsend I., Webster M.F., Simulation of cable-coating viscoelasticflow with coupled and de-coupled schemes, J. Nonnewton. Fluid Mech., 1998, 74, 1-23.
[51] Kasajima M., Ito K., Post-treatment of polymer extrudate in wire coating, Appl.Polym. Symp., 1873, 20, 221-235.
[52] Winter H.H., SPE 36th ANTEC, Tech. Papers, 1977, 23, 462.
[53] Symmons G.R., Hasmi M.S.J., Pervinmehr H., Plastohydrodynamics die lesswire drawing theoretical treatments and experimental result, in: ProgressReports in Conference in Developments in Drawing of Metals, Met. Soc. London, 1992, 54-62.
[54] Baag S., Mishra S.R., Power law model in post treatment analysis of wirecoating with linearlyvariable temperature, Amer. J. Heat Mass Transf., 2015, 2, 89-107.
[55] Kim K., Kwak H.H., Park S.H., Theoretical prediction on double-layer coating in wet-on-wet optical fiber coating process, J. Coat. Technol. Res., 2011, 8, 35-44.
[56] Kim K., Kwak H.H., Analytic Study of Non-Newtonian Double Layer Coating Liquid Flows in Optical Fiber Manufacturing, Trans Tech Publ, 2012, 224, 260-263.
[57] Zeeshan, Shah R.A., Islam S., SiddiqueA. M., Double-layer Optical Fiber Coating Using Viscoelastic Phan-Thien-Tanner Fluid, New York Sci. J.,2013, 6, 66-73.
[58] Khan Z., Islam S., Shah R.A., Khan I., Gu T., Exact Solution of PTT Fluid in Optical Fiber Coating Analysis using Two-layer Coating Flow, J. Appl. Environ. Biol. Sci., 2015, 596-105.
[59] Khan Z., Islam S., Shah R.A., Flow and heat transfer of two immiscible fluids in double-layer optical fiber coating, J. Coat. Technol. Res., 2016, 13, 1055-1063.
[60] Ali F., Aamina, Khan I., Sheikh N.A., Gohar M., Tlili I., Effects of Different Shaped Nanoparticles on the Performance of Engine-Oil and Kerosene-Oil: A generalized Brinkman-Type Fluid model with Non-Singular Kernel, Sci. Rep., 2018, 8, 15285.
[61] Tlili I., Khan W.A., Ramadan K., Entropy Generation Due to MHD Stagnation Point Flow of a Nanofluid on a Stretching Surface in the Presence of Radiation, J. Nanofluids, 2018, 7(5), 879-890.
[62] Asif M., UlHaq S., Islam S., Khan I., Tlili I., Exact solution of non-Newtonian fluid motion between side walls, Results Phys., 2018, 11, 534-539.
[63] Agaie B.G., Khan I., Yacoob Z., Tlili I., A novel technique of reduce order modelling without static correction for transient flow of non-isothermal hydrogen-natural gas mixture, Results Phys., 2018, 10, 532-540.
[64] Khalid A., Khan I., Khan A., Shafie S., Tlili I., Case study of MHD blood flow in a porous medium with CNTS and thermal analysis, Case Studies Therm. Eng., 2018, 12, 374-380.
[65] Khan I., Ali Abro K., Mirbhar M.N., Tlili I., Thermal analysis in Stokes' second problem of nanofluid: Applications in thermal engineering, Case Studies Therm. Eng., 2018, 12, 271-275.
[66] Afridi M.I., Qasim M., Khan I., Tlili I., Entropy generation in MHD mixed convection stagnation-point flow in the presence of joule and frictional heating, Case Studies in Therm. Eng., 2018, 12, 292-300.
[67] Khan M.N., Tlili I., New advancement of high performance for a combined cycle power plant: Thermodynamic analysis, Case Studies in Therm. Eng., 2018, 12, 166-175.
[68] Khan M.N., Tlili I., Performance enhancement of a combined cycle using heat exchanger bypass control: A thermodynamic investigation, J. Clean. Prod., 2018, 192(10), 443-452.
[69] Khan Z.A., Ul Haq S., Khan T.S., Khan I., Tlili I., Unsteady MHD flow of a Brinkman type fluid between two side walls perpendicular to an infinite plate, Results Phys., 2018, 9, 1602-1608.
[70] Aman S., Khan I., Ismail Z., Salleh M., Tlili I., A new Caputo time fractional model for heat transfer enhancement of water based graphene nanofluid: An application to solar energy, Results Phys., 2018, 9, 1352-1362.
[71] Khan Z., Khan I., Ullah M., Tlili I., Effect of thermal radiation and chemical reaction on non-Newtonian fluid through a vertically stretching porous plate with uniform suction, Results Phys., 2018, 9, 1086-1095.
[72] Khan I., Tlili I., Imran M.A., Fizza M., MHD fractional Jeffrey's fluid flow in the presence of thermo diffusion, thermal radiation effects with first order chemical reaction and uniform heat flux, Results Phys., 2018, 10, 10-17.

[73] Tlili I., Khan W.A., Khan I., Multiple slips effects on MHD SA-Al2O3 and SA-Cu non-Newtonian nanofluids flow over a stretching cylinder in porous medium with radiation and chemical reaction, Results Phys., 2018, 8, 213-222.

[74] Khan Z., Ur Rasheed H., Tlili I., Khan I., Abbas T., Runge-Kutta 4th-order method analysis for viscoelastic Oldroyd 8-constant fluid used as coating material for wire with temperature dependent viscosity, Sci. Rep., 2018, 8(8), 14504.

[75] Tlili I., Hamadneh N.N., Khan W.A., Thermodynamic Analysis of MHD Heat and Mass Transfer of Nanofluids Past a Static Wedge with Navier Slip and Convective Boundary Conditions, Arab. J. Sci. Eng., 2018, 1-13.

[76] Tlili I., Hamadneh N.N., Khan W.A., Atawneh S., Thermodynamic analysis of MHD Couette-Poiseuille flow of water-based nanofluids in a rotating channel with radiation and Hall effects, J. Therm. Anal. Calorim., 2018, 132(3), 1899-1912.

[77] Khan M.N., Tlili I., Khan W.A., Thermodynamic Optimization of New Combined Gas/Steam Power Cycles with HRSG and Heat Exchanger, Arab. J. Sci. Eng., 2017, 42(11), 4547-4558.

[78] Makinde O.D., Iskander T., Mabood F., Khan W.A., Tshehla M.S., MHD Couette-Poiseuille flow of variable viscosity nanofluids in a rotating permeable channel with Hall effects, J. Mol. Liq., 2016, 221, 778-787.

[79] Musmar S.A., Al-Halhouli A.T., Tlili I., Büttgenbach S., Performance Analysis of a New Water-based Microcooling System, Exp. Heat Trans., 2018, 29(4), 485-499.

[80] Ramadan K., Tlili I., Shear work, viscous dissipation and axial conduction effects on microchannel heat transfer with a constant wall temperature, Proc. Instit. Mech. Eng., Part C: J. Mech. Eng. Sci., 2015, 230(14), 2496-2507.

[81] Ramadan K., Tlili I., A Numerical Study of the Extended Graetz Problem in a Microchannel with Constant Wall Heat Flux: Shear Work Effects on Heat Transfer, J. Mech., 2015, 31(6), 733-743.

[82] Musmar S.A., Razavinia N., Mucciardi F., Tlili I., Performance analysis of a new Waste Heat Recovery System, Int. J. Therm. Envir. Eng., 2015, 10, 31-36.

[83] Shah R.A., Islam S., Siddiqui A.M., Haroon T., Wire coating analysis with Oldroy 8-constant fluid by optimal homotopy asymptotic method, Comput. Math. Appl, 2012, 63, 693-707.